Yb optical lattice clock at INRIM

D. Calonico[(1)], F. Levi[(1)], L. Lorini[(1)],G. Costanzo[(2)], M. Zoppi[(2)], M. Pizzocaro[(2)],A. Mura[(1)], E. K. Bertacco[(1)], and A. Godone[(1)]

[(1)]*Istituto Nazione di Ricerca Metrologica INRIM*
Strada delle Cacce 91, 10135 Torino, Italy
Email : d.calonico@inrim.it

[(2)]*Politecnico di Torino*
Corso Duca degli Abruzzi 24, 10129 Torino, Italy

INTRODUCTION

The Unit of Time in the International Systems of Units is realized at the relative frequency accuracy level of few parts in 10^{-16} by laser cooled Cesium fountains [1]; since 2003 INRIM has operated a laser cooled Cesium fountain with relative frequency accuracy at the level of 5×10^{-16} and has contributed with this frequency standard to the generation of the International Atomic Timescale of Bureau International des Poids et des Mesures (BIPM). Since 2009 a cryogenic Cesium fountain is under operation and its metrological characterization is in progress, with a target accuracy of 1×10^{-16}.

The current realization of the second is expected to be improved in the next future by high performances optical clocks as regognized by time and frequency community, by the BIPM and the Time and Frequency Consultative Commitee of the International Committee for Weights and Measures, and in the future a possible redefinition of the second could be based also on optical atomic transitions.

In order to go beyond the relative frequency accuracy level of 1×10^{-16}, several laboratories have developed or are developing optical frequency standards based on neutral atoms [2-6] or ions [7-9], and outstanding results have been obtained with frequency uncertainties of few parts in 10^{-16} and even few parts in 10^{-17} in the comparison between Hg^+ and Al^+ frequency standards.

In this scenario, INRIM has started the developement of a lattice optical clock based on neutral Ytterbium, as it is a recognized candidate for optical clock realizations, and high-performances Yb optical frequency standards have beeen demonstrated at National Institute of standards and Technology both on the even isotope 174 and the odd 171 [10, 11].

The Ytterbium clock reference transition $^1S_0 \rightarrow ^3P_0$ ($\lambda = 578.4$ nm) is strictly dipole-forbidden from spin and orbital angular momentum selection rules; an appreciable excitation probability is present for odd isotopes due to hyperfine state mixing of the $^3P_0$ sublevels resulting in a natural linewith of $\sim$ 10 mHz; for even isotopes the clock transition could be excited by Magnetic Induced Specrtoscopic techniques [12].

The clock transition is ac-Stark shift free when Ytterbium is trapped in a dipole far off resonance lattice at the magic wavelength of 759 nm.

Laser cooling of Ytterbium is obtained by a double stages magneto-optical trap. First, using the dipole transition $^1S_0 \rightarrow ^1P_1$ at 399 nm (natural linewidth Γ = 28.9 MHz), whose Doppler limit temperature is 690 μK. Then, atoms can be furtherly cooled using the intercombination line $^1S_0 \rightarrow ^3P_1$ at 556 nm (completely closed, Γ = 187 kHz), whose Doppler limit is 4.5 μK. Then, cold Ytterbium can be trapped in the optical lattice with an efficiency of about 10%.

Yb also provides the possibility for studing bosonic, fermionic and mixed systems, having five bosonic isotopes and two fermionic ones. The atomic levels scheme is reported in Fig.1.

EXPERIMENTAL SET UP

In our experimental set up, the atomic Yb source is an effusion oven operating between 360 and 390°C, the nozzle is multichannel array realized with a microtubes bundle, maintained at a temperature of 400°C. The latter is made by 200 microtubes in Monel400 (100 μm of internal diameter, 10 mm long), that implies a thermal beam divergence of 17 mrad. The physical structure is mantained under Ultra High Vacuum by two ion pumps which ensures a differential vacuum: the trap region is mantained at10^{-6} Pa and the oven region pressure is ten times higher. The MOT region is placed about 50 cm from the nozzle, where the thermal beam has a diameter of 20 mm. There is not a Zeeman slower in order to

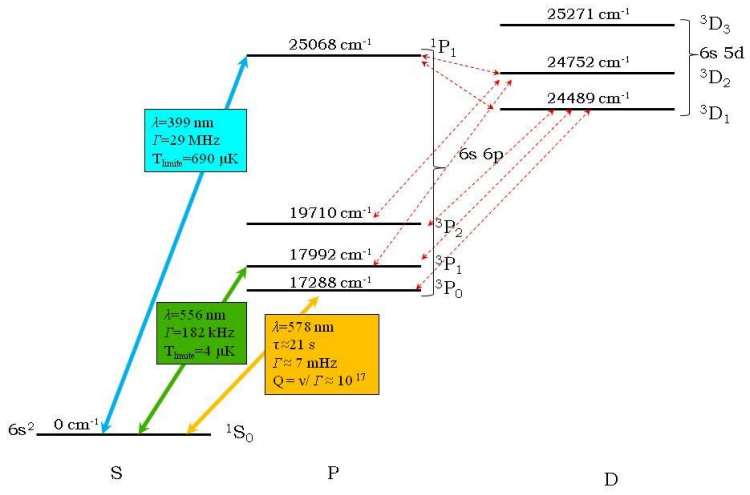

Fig. 1. Yb energy levels.

simplify the structure and avoiding any stray magnetic field in the clock implementation. Yb atoms interacts with three retro-reflected laser beams in a XYZ (0,0,1) configuration, each beam has 4 mm diameter and is red detuned of about 14 MHz. Two double-pass acusto-optic modulator systems[14] are used to frequency detune the laser frequencies. The MOT magnetic static gradient is generated by two anti-Helmholtz coils that provide a magnetic field gradient of 12 gauss/cm/A. The trapped atoms cloud is approximately spherical and has a diameter of 1 mm (1/*e*, for the 399 nm MOT). Atomic fluorescence light is collected by a CCD camera placed outside the vacuum chamber, 25 cm far away from the interaction region.

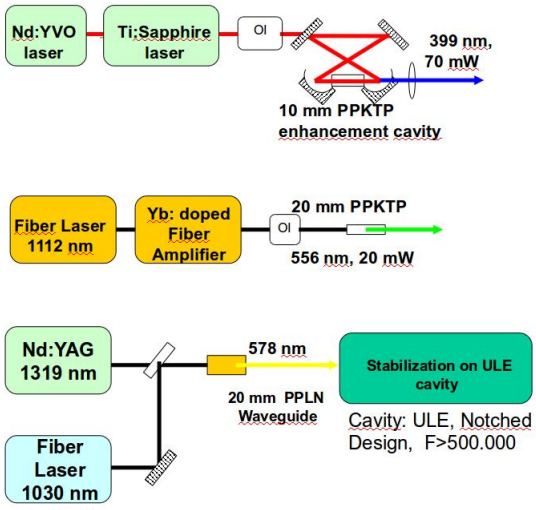

Fig. 2. Optical bench scheme for the experiment laser generation.

In order to increase the number of atoms in the trap an additional cooling laser beam, counterpropagating to the Yb beam, has been added: this beam works at a fixed frequency, which is 140 MHz red detuned from the atomic resonance of the 399 nm transition for each isotope and, currently, its intensity is comparable to the one of the 399 nm cooling beams.

In our experimental setup, the laser radiation at 399 nm is provided by the 798 nm radiation obtained from a Ti-Sa laser frequency doubled using a 20 mm long PPKTP crystal placed in an enhancement ring cavity. Up to 70 mW of 399 nm radiation have been obtained from 600 mW infrared radiation. The resonant ring cavity is locked to the Ti-Sa laser using the Hänsch-Couillaud technique [15].

The 556 nm radiation is generated by frequency doubling of a 1112 nm source generated by a Yb:doped fiber laser and a fiber amplifier. A PPKTP crystal in a single pass configuration provides up to 20 mW of 556 nm radiation from 1 W infrared laser radiation.

The clock radiation at 578 nm will be generated using the Sum Frequency Generation in a 20 mm long PPLN waveguide non linear crystal pumped by a 100 mW ND:YAG laser at 1319 nm and a 93 mW Er:doped fiber laser at 1030 nm, whose radiation will be mixed in a fiber coupler and iniected in the crystal. The clock radiation will be stabilized using an ultra-stable ULE cavity whose finesse is expected to be about 200000 with a notched design in order to use as supports the Airy points of the cavity[25]. The optical bench scheme is reported in Fig. 2.

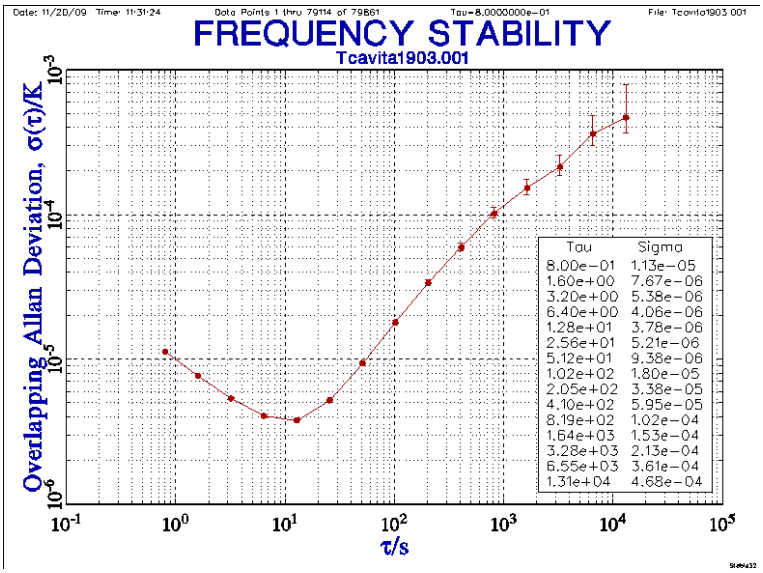

Fig. 3. Temperature stability of the ULE cavity.

In order to minimize the perturbation from the enviroment, the ULE cavity is closed in a vacuum chamber thermally controlled where the pressure is mantained at a constant level of 10^{-4} Pa by a 2 l/s ion pump. The vacuum chamber is placed on an vibration insulation platform to reduce the seismic noise and closed in a acoustic enclosure. The thermal control of the chamber allows to search for the zero-CTE temperature of the cavity, that is between 20 and 40 °C at 90% confidence level. The temperature stability is shown in Fig. 3 This stability, better than 1 μK at 1 s is compatble with a frequency stability of 10^{-15} at 1 s.

The seismic noise limitation to the final frequency stability has been evaluated by use of a Finite Elements Modelling software. In the experiment configuration, a frequency stability of 10^{-15} at 1 s is achievable if the seismic noise presents a root mean square acceleration $\leq 2.5 \times 10^{-4} m \cdot s^{-2}$. The seismic noise spectrum has been measured by a seismometer on the acoustic enclosure floor and on the cavity dumped board and the results are reported in Fig. 4. Within 100 Hz, the equivalent acceleration is $\leq 1 \times 10^{-4} \mathrm{m} \cdot \mathrm{s}^{-2}$.

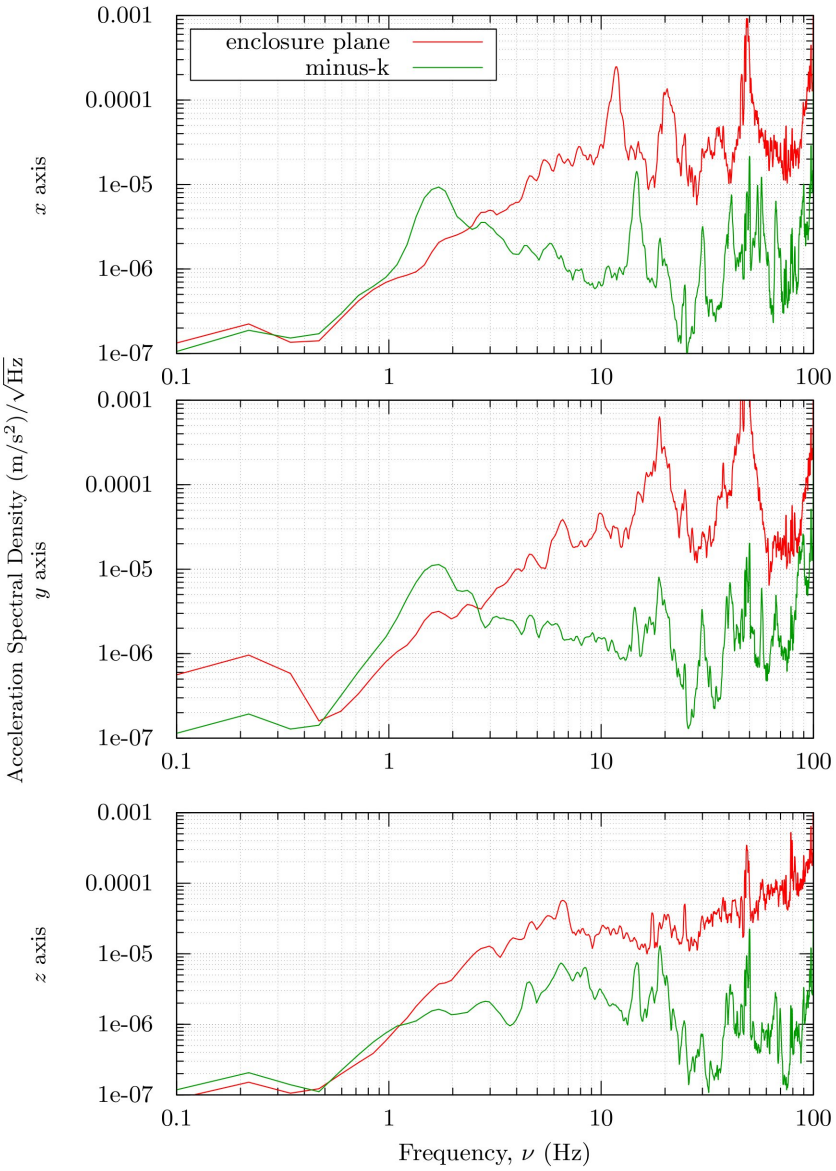

Fig. 4. Seismic noise on the ULE cavity dumped board

MEASUREMENTS OF THE $^1P_1$ BRANCHING RATIOS

Currently, atoms have been cooled in the 399 nm MOT and five isotopes have been trapped; a typical image is reported in Fig. 5. A first study concerns the dynamics of the number of atoms in the trap, analyzing the loading curve of the trap for different isotopes. First of all we have evaluated the number of atoms, analizing the fluorescence light collected by the CCD camera and using the relation Eq.1:

$$P_{MOT} = P_{MOT,tot}\frac{\Omega}{4\pi}a_{shut}T = \frac{hc}{\lambda}N_{atoms}\left(\frac{\Gamma}{2}\frac{I/I_0}{1+I/I_0+(2\delta/\Gamma)^2}\right)\frac{\Omega}{4\pi}a_{shut}T \qquad (1)$$

where P_{MOT} is the light power collected by the CCD camera, δ is the detuning of the laser beams, I_0= 60 mW/cm^2 is the saturation intensity for the 399 nm transition, I the total beam intensity of the six laser beams in the trap, $\Gamma = 2\pi\times$ 28.9

MHz is 2π times the linewidth of the transition, $\frac{\Omega}{4\pi}$ the solid angle substained by the CCD camera, a_{shut} a corretion factor due to the mechanical shutter of the CCD camera and T the transmittance of the windows of the vacuum chamber.

The typical intensity of each laser beam is about $5 \div 8$ mW cm^{-2}, obtaining a total intensity in the trap $\sim (0.5 \div 0.8) I_0$: $3 \cdot 10^5$ atoms can be trapped without the pre-cooler and up to $1.5 \cdot 10^6$ with the pre-cooler, whose intensity is equivalent to those of the trapping beams. This result makes possible to avoid a Zeeman slower in the setup. Image Analysis of CCD camera signal shows that the density distribution of the atoms in the trap is well described by a gaussian function, as shown in Fig. 6.

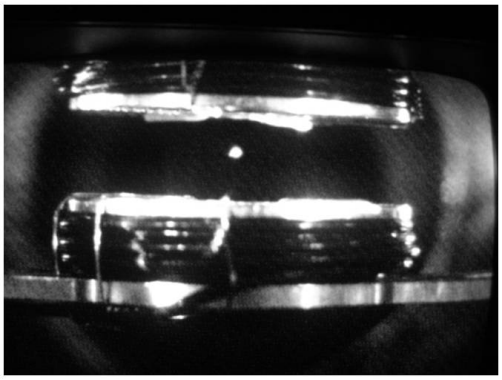

Fig. 5. Yb MOT atomic trap atoms fluorescence; the coils for the magnetic static gradient generation are visible.

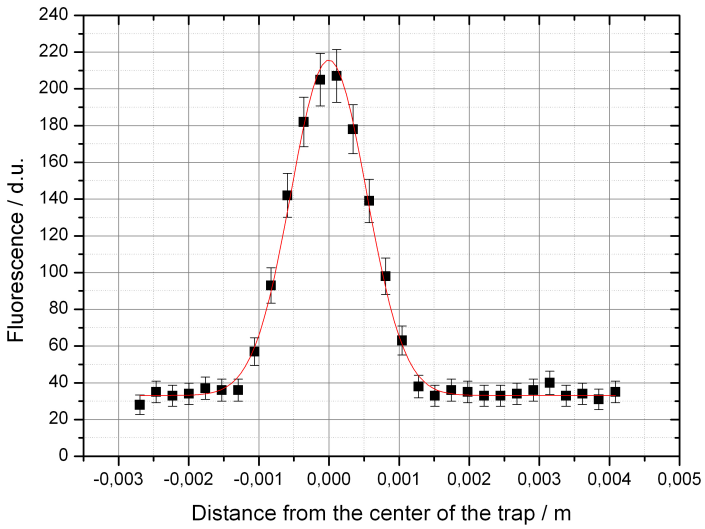

Fig. 6. The Gaussian profile of the atomic cloud in the MOT.

The maximum central value of the density n_0 currently reached is $4 \cdot 10^8$ cm^{-3} with a diameter of 1 mm.
The time evolution of the number of the atoms in the trap can be described as [18]:

$$\frac{dN}{dt} = R - \alpha N - \beta \int n^2(\vec{r}) d^3\vec{r} \qquad (2)$$

where R is the trap capture rate, α the linear loss rate, β the rate coefficient for two body collisions and r the internuclear distance, $n(\vec{r})$ the spatial density distribution. As shown in Fig. 5, the spatial distribution of the atom density in the trap is gaussian and it can be written as $n(\vec{r}) = n_0 e^{-|\vec{r}|^2/a^2}$, so the last integral can be evaluated, obtaining the expression:

$$\frac{dN}{dt} = R - \alpha N - \frac{\beta}{(\sqrt{2\pi}a)^3} N^2 \qquad (3)$$

In the following calculations, only the linear term will be considered, so the solution of the differential equation is $N(t) = R\tau\left(1 - e^{-\frac{t}{\tau}}\right)$ with $\tau^{-1} \equiv \alpha$, that defines the loading time of the trap. According to a simple model, it is possible to write the trap loading time separating the contribution to the loss of the trap due to the collisions with the atoms from the thermal beam and the contribution due to the de-excitation of the atoms from the $^1P_1$ state to the metastable states $^3P_{2,0}$ via the D-states $^3D_{2,1}$. Assuming that the collisions with different species of isotopes are negligible, the trap loading time is:

$$\tau_{is}^{-1} = \eta_{is} L + a_{2,0} f \qquad (4)$$

where τ_{is}^{-1} is the laoding time for the *is* isotope, η_{is} its abundance, L a term which inludes all the contribution linear in the abundance, f the fraction of the atoms in the excited state, defined as

$$f \equiv \frac{1}{2} \frac{I/I_0}{1 + I/I_0 + (2\delta/\Gamma)^2} \qquad (5)$$

According to assumptions made, the meaning of the term L is the following: the rate of the atoms ejected from the trap by collisions with atoms in the thermal beam can be written as $\alpha_b = n v_{th} \sigma$, where n is the density of the atoms of the background, v_{th} the thermic velocity (the same within the 2% for all the isotopes) and σ the cross section for collisions with the same isotope, which can be assumed to be approximately constant for all the isotopes (a simple classical model calculates that the dependence from the isotope is $\propto M^{1/6}$, so the discrepancy is less than 1%). Writing $n = \eta_{is} n_{tot}$, with n_{tot} the density of all the isotopes in the thermal beam, we obtain $\alpha_b = \eta_{is} L$.

A typical experimental loading curve obtained is presented in Fig. 7.

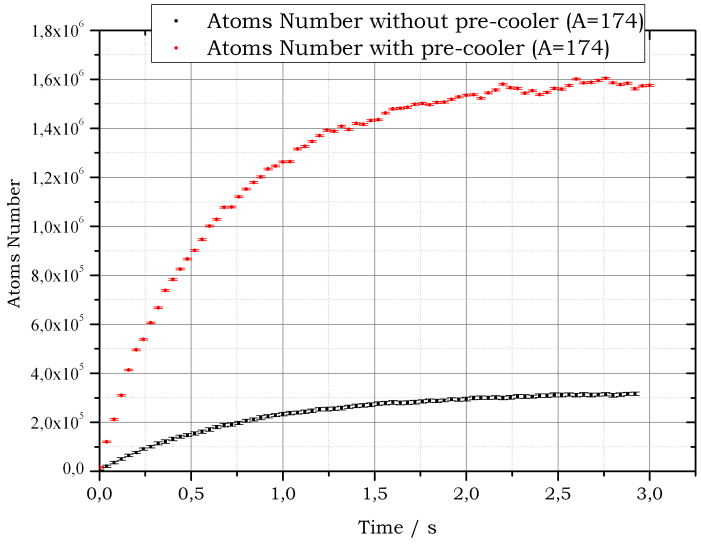

Fig. 7. Loading signal in the ^{174}Yb 399 nm MOT, with and without the pre-cooler beam.

As already observed in [17], the presence of the pre-cooler introduces an additional loss channel not well predictable, so all these acquisition were made without the pre-cooler beam (this is the reason because the intensity of the pre-cooler beam is maintained similar to the trapping ones). The loading curves acquired for the isotopes 170 and 171 were too noisy, so all the calculations were made using the three most abundant bosonic isotopes, that is A = 172, 174, 176. The measured value of the lifetime of the three most abundant bosonic isotopes are reported in Table 1.

Isotope	τ /ms	Abundance %
172	852(7)	21.9
174	801(6)	31.8
176	78(6)	12.7

TABLE 1. Measured loading times for the three most abundant bosonic isotopes

Comparing the loading times of the three possible couples of isotopes, we can construct three different simple linear system with unknown quantities L and $a_{2,0}$ and the results for $a_{2,0}$ are reported in Tab.2. The uncertainity of the results is mainly due to the incomplete knowledge of the intensity of the laser beam in the trap itself and to estimate this lack of knowledge we adopted a cover factor equal to the 30% of the total value of the laser intensity.

Isotope 1	Isotope 2	a_{20}This Work	a_{20} Ref. [18]	a_{20} Ref. [19-24]
172	174	8(4) s^{-1}		
172	176	10(5) s^{-1}	23(11) s^{-1}	6.6(4.6)s^{-1}
174	176	11(5) s^{-1}		

TABLE 2. Branching ratio a_{20} for the decay of the $^1P_1$ state to the metastable states $^3P_{2,0}$ via the D-states $^3D_{2,1}$

In Tab.2 are also reported the value of $a_{2,0}$, evaluated by [18] from the intensity dependence of the lifetimes, and the theoretical prediction for this branching ratio [19, 20, 21, 22, 23, 24]. The value obtained from our measurement agrees with the theory and also with the experimental value [18], even if in our model an important assumption about the collisional rate was made, in order to justify the differences in the loading times.

CONCLUSIONS AND PERSPECTIVES

At INRIM, the development of an Ytterbium lattice clock is in progress. Up to now, the experiment is capable of trapping and cooling five Yb isotopes using the allowed transition at 399 nm, without the use of any Zeeman slower, and then demonsrating the possibility to implement a simpler physicis package for neutral atoms optical clock. Indeed, the use of just a fixed frequency precooling laser, generated by the same cooling lasers, allows the loading of $1.5{\cdot}10^6$ atom, that are enough to implement the optical clock. The branching ratio $a_{2,0}$ has been measured, in fair agreement with theoretical predictions and with previous measurements. The clock radiation will be provided by sum frequency generation in a waveguide crystal and stabilized on an ultrastable ULE cavity. The ULE cavity reference has already been realized and its length thermal and seismic noise has been characterized, demonstrating not to be a limit to reach a relative frequency instability of parts in 10^{-15} over 10 s integration time.

ACKNOLEDGEMENTS

This work is supported by Regione Piemonte (YTRO Project) and by the European Metrology Research Programme (EMRP) through the execution iMERA-Plus of Euramet (OCS T1J2.1 Project).

REFERENCES

[1] T. E. Parker, Long-term comparison of caesium fountain primary frequency standards . *Metrologia*, 47 (2010) 1–10;
[2] M. M. Boyd et al., 87Sr Lattice Clock with Inaccuracy below 10-15, Phys. Rev. Lett. 98, 083002 (2007);
[3] A. D. Ludlow et al., Sr Lattice Clock at 1 x 10–16 Fractional Uncertainty by Remote Optical Evaluation with a Ca Clock, Science 319, 1805 (2008);
[4] X. Baillard et al. An optical lattice clock with spin-polarized 87Sr atoms Eur. Phys. J. D 48, 11–17 (2008);
[5] Ch. Lisdat et al. Collisional Losses, Decoherence, and Frequency Shifts in Optical Lattice Clocks with Boson Phys. Rev. Lett. 103, 090801 (2009);
[6] M. Petersen, et al. Doppler-Free Spectroscopy of the 1S0-3P0 Optical Clock Transition in Laser-Cooled Fermionic Isotopes of Neutral Mercury Phys. Rev. Lett. 101, 183004 (2008)

[7] T. Rosenband et al., Frequency Ratio of Al+ and Hg+ Single-Ion Optical Clocks; Metrology at the 17th Decimal Place Science 319, 1808 (2008);
[8] T. Schneider, et al., Sub-Hertz Optical Frequency Comparisons between Two Trapped 171Yb+ Ion Phys. Rev. Lett. 94, 230801 (2005);
[9] G. P. Barwood et al. Measurement of the Electric Quadrupole Moment of the 4d 2D5/2 Level in 88Sr +, Phys. Rev. Lett. 93, 133001 (2004)
[10] N. D. Lemke et al. Spin-1/2 Optical Lattice Clock, Phys. Rev. Lett. 103, 063001 (2009)
[11] C. W. Hoyt et al., Observation and Absolute Frequency Measurements of the 1S0-3P0 Optical Clock Transition in Neutral Ytterbium Phys. Rev. Lett. 95, 083003 (2005)
[12] Z. W. Barber et al., Direct Excitation of the Forbidden Clock Transition in Neutral 174Yb Atoms Confined to an Optical Lattice , Phys. Rev. Lett. 96, 083002 (2006)
[13] S. G. Porsev, A. Derevianko and E. N. Fortson, Possibility of an optical clock using the $6^1S_0 \rightarrow 6^3P_0$ transition in ^{171,173}Yb atoms held in an optical lattice *Phys. Rev. A*, **69**, 021403R (2004).
[14] E. A. Donley et al., *Double-pass acousto-optic modulator system Rev. Sc. Instr.*, **76**, 063112 (2005).
[15] T. Hänsch, B. Couillaud, *Laser frequency stabilization by polarization spectroscopy of a reflecting reference cavity, Opt. Commun.*, **35**(3), 441 (1980).
[16] T. P. Dinneen, et al., Cold collisions of Sr*-Sr in a magneto-optical trap *Phys. Rev. A*, **59**, 1216 1999).
[17] R. L. Cavasso-Filho, et al., Observing negligible collision trap losses: the case of alkaline-earth metals *Phys. Rev. A*, **67**, 021402(R) (2003).
[18] T. Loftus, et al., Power-dependent loss from an ytterbium magneto-optic trap *Phys. Rev. A*, **61**, 051401(R) (2000).
[19] W. C. Martin, R. Zalubas, *Atomic energy levels, The rare earth elements*, NSRDS-NBS 60 (1978).
[20] J. Migdalek and W. E. Baylis, Relativistic transition probabilities and lifetimes of low-lying levels in ytterbium *J. Phys. B.***24**, L99 (1991).
[21] D. Demille, Parity Nonconservation in the Transition in Atomic Ytterbium *Phys. Rev. Lett.* **74**, 4165 (1995).
[22] C. J. Bowers et al., Experimental investigation of excited-state lifetimes in atomic ytterbium *Phys. Rev. A* **53**, 3103 (1996).
[23] C. J. Bowers et al., Experimental investigation of the forbidden transitions in atomic ytterbium *Phys. Rev. A* **59**, 3513 (1999).
[24] S. G. Porsev, Y. G. Rakhlina and M. G. Kozlov, Electric-dipole amplitudes, lifetimes, and polarizabilities of the low-lying levels of atomic ytterbium *Phys. Rev. A* **60**, 2781 (1999).
[25] From an original idea of T. Rosenband (NIST).